A comparison of the structure of N2 and CO2 diluted CH4/O2 premixed flames in a swirled combustor

P. Jourdaine[a,b,c,*], C. Mirat[a,b], J. Beaunier[a,b], Y. Joumani[c], T. Schuller[a,b]

[a]*Ecole Centrale Paris*
Grande Voie des Vignes, 92295 Châtenay-Malabry, France
[b]*CNRS, UPR 288 Laboratoire d'Energétique Moléculaire et Macroscopique, Combustion (EM2C)*
Grande Voie des Vignes, 92295 Châtenay-Malabry, France
[c]*Air Liquide, R&D Paris Saclay, 1 Chemin de la porte des Loges, 78354 Jouy-en-Josas, France*

Abstract

Oxygen enhanced natural gas combustion with flue gas recirculation is envisaged as an alternative of air combustion technologies to ease the capture and sequestration of CO_2. In this study, effects of N_2 replacement by CO_2 are examined for diluted lean premixed swirled CH_4/O_2 flames aerodynamically stabilized at the dump plane of a generic combustor. Effects of the injector quarl, swirl, adiabatic flame temperature, laminar burning velocity and injection bulk velocity on the stabilization and the topology of these flames are analyzed. The swirl number and the quarl angle have a major impact on the flame topology. Changing the swirl number allows to easily obtain successively V-, M- or tulip-shaped flames. Quarl allows to widen the range of operation. Differences between N_2 and CO_2 diluted flames are highlighted.

Introduction

This study is part of the OXYTEC project developed in collaboration between Air Liquide and EM2C laboratory to improve the knowledge on oxycombustion. One of the objectives is to promote the development of combustion technologies with reduced CO_2 emission levels from industrial plants. Oxycombustion is a way to improve combustion efficiency [1] and has already been combined with carbon capture and storage technologies at the highest technological readiness level [2].

One difficulty is to revamp existing air powered furnaces with oxyburners with a limited number of modifications and without impairing performances and emissions. The characteristics of oxyflames should be known in order to reproduce similar conditions in the furnace as those obtained with conventional air operated burners. Otherwise, the furnace could eventually be damaged, its life duration may be shortened or the process may be altered. Since oxygen separation from air represents the largest share of electricity consumption in oxyfuel plants [3], oxyburners are generally operated at lean conditions but very near stoechiometry and dilution is used to lower the temperature of the burnt products [4]. Comparisons between oxy-diluted- and air-powered flames need thus to be carried out.

The main parameters controlling the shape of premixed swirled oxy-flames diluted by CO_2 are analyzed in this study. Effects of the swirl number, S, have already received a considerable attention (see for examples [5, 6, 7] or more recently [8]). It is known that for a critical threshold of about $S \sim 0.6-0.7$, that slightly depends on the injector and combustion chamber geometries and on the flow operating conditions, an internal recirculation zone filled with burnt products takes place along the burner axis allowing to aerodynamically anchor swirled flames relatively far away from all solid elements. The impact of geometrical elements from the combustor has also been investigated [7, 9, 10]. The confinement and the quarl angle at the burner outlet are the main parameters affecting the flame topology. It was also found that the confinement modifies the thermal conditions inside the combustor. These studies are however rarely conducted with CO_2 diluted flames.

The fundamental properties of CO_2 diluted laminar oxy-flames have been investigated in a serie of studies. It is found that dilution by CO_2 decreases faster the laminar burning velocity than N_2 dilution [11, 12]. Unlike N_2, CO_2 is chemically active [13], that partly explains the decrease of the laminar burning velocity with CO_2 dilution. Liu *et al.* [14] did detailed chemical kinetics and thermodynamic calculations of $CH_4/O_2/CO_2/H_2O$ flames under conditions relevant to gas turbine operations. They showed that for stoechiometric combustible mixtures at high pressure, a good oxygen/diluent ratio needs to be selected otherwise the flame will be blown off or it will be too hot for its industrial use. Effects of CO_2 addition on the extinction limits of the flame have also been studied. Jung *et al.* [15] showed that for a premixed flame, the flame stability map was reduced compared to a N_2-diluted flame. Kobayashi *et al.*[16] investigated effects of CO_2 dilution for premixed turbulent CH_4/air jet flames. They found that addition of CO_2 decreases the turbulent flame speed, increases the flame volume and restrains combustion oscillation especially at high pressure.

Comparisons between $CH_4/O_2/N_2$ and $CH_4/O_2/CO_2$ flames have also been carried out in combustors with swirled injectors. Schroll *et al.* [17] compared the dynamic stability of a $CH_4/O_2/N_2$ and $CH_4/O_2/CO_2$ flame in a premixed swirled combustor. They found that for Reynolds numbers $Re < 25000$ based on the bulk

*Corresponding author: paul.jourdaine@ecp.fr

flow injection velocity and injector diameter, the shape of the flame is controlled by the adiabatic flame temperature and that for the same adiabatic temperature and the same Reynolds number CO_2-diluted and N_2-diluted flames have the same topology. Seepana *et al.* [18] worked on a co-axial swirled burner. They showed that for oxycombustion diluted by CO_2, a higher oxygen concentration of around 33-34% by volume in the oxidizer is needed to get temperature profiles similar to those measured when the combustor is operated with air. Their experiments also indicate that $CH_4/O_2/CO_2$ flames are more susceptible to be quenched than $CH_4/O_2/N_2$ flames. Amato *et al.* [19] also found that the operability boundaries of a swirl premixed combustor with a bluff-body powered by $CH_4/O_2/CO_2$ combustible mixtures are significantly reduced compared to $CH_4/O_2/N_2$ fuel blends. For the same power and adiabatic flame temperature, N_2-diluted flame is stable at a lower equivalence ratio than CO_2-diluted flame. Lee *et al.* [20] studied radiative effects of CO_2 on premixed flame stabilization. They found that the substitution of N_2 by CO_2 leads to a reduction of the temperature in the combustor. This reduction is due to the higher thermal capacity of CO_2 and to the thermal radiation from CO_2.

This brief review indicates that the topology of $CH_4/O_2/CO_2$ swirled premixed flames depends on the geometry of the combustor and especially on the angle of the quarl at the burner outlet, the swirl number S, the adiabatic flame temperature T_{ad}, the Reynolds number Re of the flow in the injector, the bulk injection velocity U_b and the laminar burning velocity S_L. Heat losses also impact a role in the shape of confined swirled flames [21, 22], but these second order phenomena are not considered in the following experiments. Observations are reported on effects of these parameters on the shape taken by aerodynamically stabilized swirled flames diluted by N_2 and CO_2. A high pressure test rig has been developed to this purpose. First results obtained at atmospheric pressure for CO_2-diluted CH_4/oxy-flames and CH_4/air flames are presented. The OH^* chemiluminescence signal is used to investigate the impact of dilution on flame shape and stability.

Experimental setup

Figure 1(a) shows the injector and the combustion chamber of the OXYTEC test rig that has been designed to investigate oxycombustion diluted by CO_2 and/or H_2O up to 30 bar and with a thermal power limited to 200 kW. In the present work, the high pressure combustion chamber has been replaced by an atmospheric chamber shown in Fig. 1(b). This chamber has the same internal geometry as the high pressure chamber. It is a parallelepiped with a 150 mm square cross section and 250 mm height equipped with four quartz windows allowing a large optical access to the flame. A convergent at the top is used to reduce the outlet section by 20%. Simulations with Ansys Fluent showed that this section reduction allows to fix the recirculation zones fo the flow inside the combustion chamber without ambient air entrainment from the surrounding. This atmospheric rig is operated with the same burner as the high pressure rig.

Figure 1(c) shows a disassembled view of the injector. The outlet diameter of the burner is $D = 20$ mm. The swirl is produced with an axial-plus-tangential entry swirl generator ([7], p. 168). This injector allows to continuously change the swirl number S during the experiments by modifying the ratio of the mass flow rates injected tangentially $\dot{m}_\theta$ and axially $\dot{m}_z$:

$$S = \frac{HR\pi}{2lLN}\frac{1}{1+\dot{m}_z/\dot{m}_\theta} \quad (1)$$

where H is the distance separating the azimuthal injection channels from the burner axis, R is the injector outlet radius, l and L are the width and the height of the N injection azimuthal channels. This device was designed to produce swirl numbers ranging from $S = 0$ to 1.75.

Pur methane is mixed with the oxidant and CO_2/N_2 diluents inside the tangential slits of the swirler by a set of holes for a rapid and good mixing. The combustible mixture leaves the swirler and flows out into the combustion chamber through an end piece eventually equipped with a quarl (Fig. 1(d)). Quarls with angles $\alpha = 10°, 30°, 45°$ and $60°$ can be placed on the top of the swirl generator. The combustion chamber flange, which is in contact with the burnt gases is cooled by water circulation.

Table 1 summarizes the operating conditions investigated in this study. The adiabatic flame temperature T_{ad} and laminar burning velocity S_L are calculated with a home made solver REGATH [23] run with the GRI 3.0 mechanism [24]. In all experiments, the combustible mixture is injected at ambient temperature, care was taken to thermalize the injection lines of the different gases and measurements were all realized five minutes after ignition. Bronkhorst mass flowmeters are used to control the different flow rates injected. Dilution is characterized by the percentage of CO_2 or N_2 in the oxydant:

$$X_{N2} = \frac{n_{N2}}{n_{N2}+n_{O2}} \quad X_{CO2} = \frac{n_{CO2}}{n_{CO2}+n_{O2}} \quad (2)$$

where n_i denotes the number of moles of species i.

A 12 bit intensified CCD camera (Princeton, PI-MAX, 512×512 pixels^2) with an UV objective (Nikkor 105 mm) and a pass band filter center at 308 nm (Melles-Griot F10-307.1-4-50.0M) were used to record the OH^* chemiluminescence signal from the combustion region. This signal is a good tracker of the reaction zone for premixed flames [25]. The flame topology is examined by recording average pictures of the turbulent reacting flow. The average images were built from the accumulation of 30 snapshots with a camera gate width of 25 ms. Dimensions in Figs. 2, 3, 4, 5, 6 and 7 are in mm. An Abel

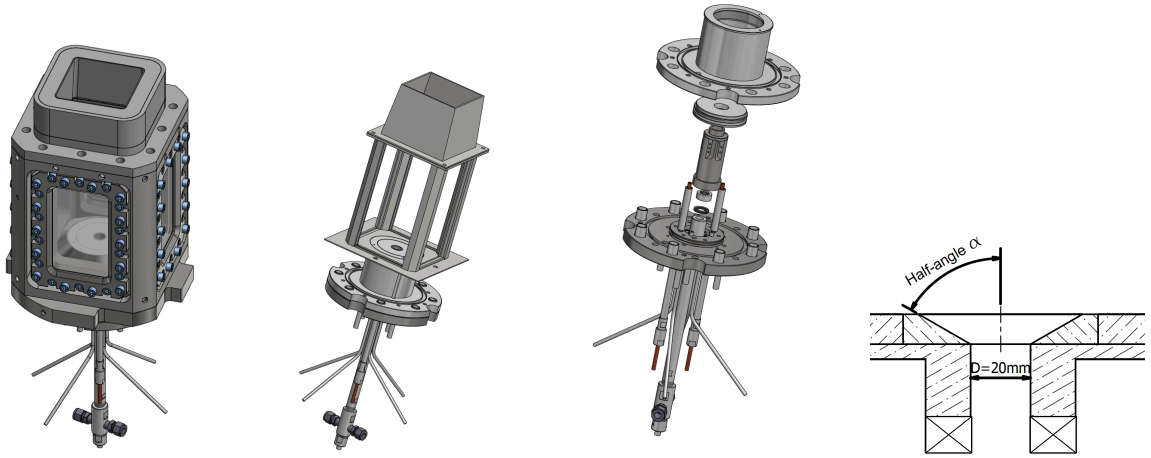

(a) Oxytec high pressurecombustion chamber with the injector (b) Oxytec atmospheric pressure chamber with the injector (c) Diasassembled view of the injector (d) Schematic view of the injector

Figure 1: Views of the Oxytec chambers and the injector

Table 1: Injection conditions

	P (kW)	ϕ	S_L (cm/s)	U_b (m/s)	U_b/S_L	X_{dil}	T_{ad} (K)	S
CO2	10-20	0.7-1	13-21	7-18	34-75	0.66-0.70	1900-2200	0.5-1.2
N2	5-20	0.7-1	5-37	10.5-25	14-105	0.79-0.84	1850-2200	0.5-1.2

transformation was also applied for some configurations where the average flame is axisymmetric. This operation yields a slice of the OH* distribution in a vertical plane of symmetry of the burner [26]. Images are then scaled in terms of volumetric heat released rate. We assume here that the relation between OH^* chemiluminescence and heat release rate is linear [27] and only depends on the equivalence ratio [28] which was maintained here at $\phi = 0.95$ for most of the conditions explored.

Effects of quarl

Experiments were first carried out without quarl on the top of the swirler. It was not possible in this case to stabilize lean flames with equivalence ratios lower than $\phi < 0.8$. To lower the lean blow off limit, a divergent quarl was added on the top of the burner to help flame stabilization (Fig. 1(d)). A parametric study was conducted to select the best value for the quarl angle $\alpha = 10°$, 15°, 45° or 60°. The height of the quarl was fixed following guidelines from Gupta ([7], p. 288) $H_{quarl} = 0.5D$.

Figure 2 shows flames obtained for the different divergent quarls at the same injection conditions. With a large angle, $\alpha = 45°$ and 60°, flames stabilize close to the burner outlet very close to the combustor dump plane or inside the injector even at a low swirl number S. These flames are not desired because they will eventually damage the burner or lead to too high thermal stress in the final application. For a smaller angle $\alpha = 15°$, it was possible to stabilize flames with V- or M- or tulip-like-shapes near the burner lips or with a V-shape lifted above the burner outlet. For $\alpha = 10°$, it was easier to stabilize lifted flames above the injection unit allowing a full optical access to the combustion region. To make the larger study possible, we decided to work with this quarl.

Effects of swirl number

Figure 3 shows the structure of $CH_4/O_2/CO_2$ flames for different swirl numbers. When $S = 0.7$, the flame is highly turbulent and lifted far away above the burner. The shape of the flame is difficult to define. It is stabilized in one corner of the combustion chamber, because the flow is not entirely symmetric inside the chamber. Between $S = 0.8$ and $S = 0.9$, the flame takes a V or a M-shape [29, 22]. When $S = 1.0$, the flame shape changes again to become a tulip-flame [30]. For higher swirl numbers, $S > 1$, the flame keeps a tulip shape until the flame is lifted far away above the injector. In this case, the flame is again highly turbulent and its shape is difficult to define.

Flames for $S \leq 0.7$ and $S \geq 1$ are not studied, because they strongly interact with the combustion chamber walls and are highly unsteady. They are not interesting from a practical point of view. For $S \simeq 0.75$, a V-shape flame lifted above the burner is observed. The range of swirl numbers S where this stabilization regime takes place depends on the injection bulk flow velocity U_b and thermal power P. This stabilization regime widens when U_b or P increase.

The same experiments were repeated for $CH_4/O_2/N_2$ flames at the same thermal power $P = 12.5$ kW, equivalence ratio $\phi = 0.95$ and adiabatic flame temperature. Results were almost identical. The transition regimes of the different shapes taken by the swirled flames appear nearly at the same swirl numbers S for N_2- and CO_2-diluted flames investigated. Only transitions where the

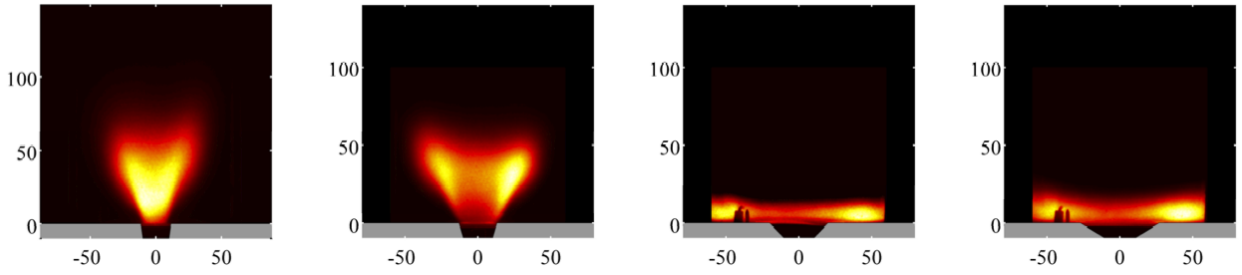

(a) α= 10° (b) α= 15° (c) α= 45° (d) α= 60°

Figure 2: CH_4/air flames $\phi = 0.95$, $S = 0.9$, $P = 12.5$ kW, with different quarl angle α

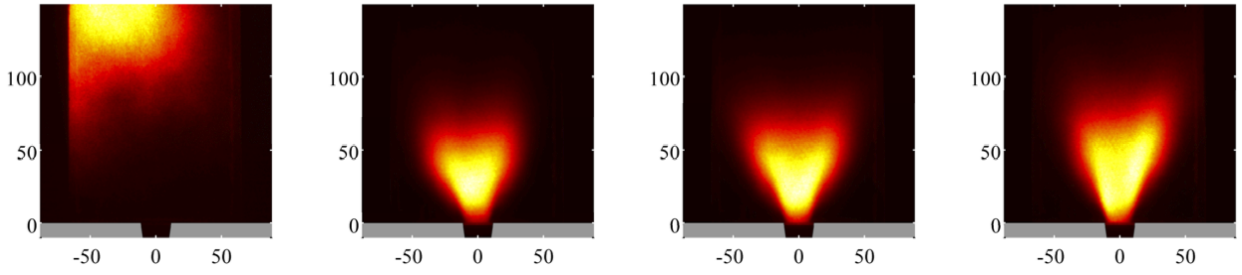

(a) $S = 0.7$ (b) $S = 0.8$ (c) $S = 0.9$ (d) $S = 1.0$

Figure 3: $CH_4/O_2/CO_2$ flames $X_{CO_2} = 68\%$, $\phi = 0.95$, $P = 12.5$ kW, $\alpha = 10°$ and varying swirl numbers S.

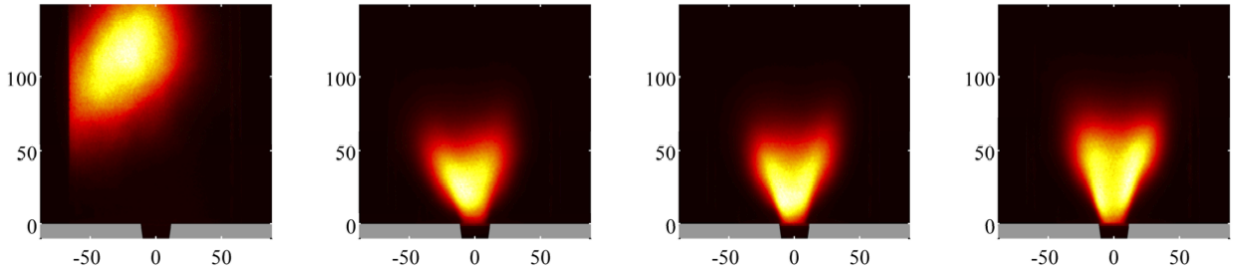

(a) $S = 0.7$ (b) $S = 0.8$ (c) $S = 0.9$ (d) $S = 1.0$

Figure 4: CH_4/air flames $\phi = 0.95$, $P = 12.5$ kW, $\alpha = 10°$ and varying swirl numbers S.

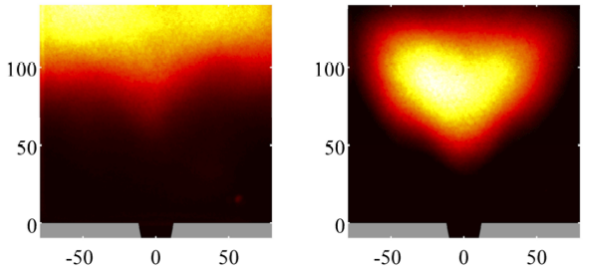

(a) X_{N_2}=0.83, ϕ=0.95, S=0.8, P=15 kW, U_b/S_L=93.2 (b) X_{N_2}=0.79, ϕ=0.8, S=0.8, P=15 kW, U_b/S_L=66.4

Figure 5: $N_2/O_2/CH_4$ flames at the same $T_{ad} = 2010$ K

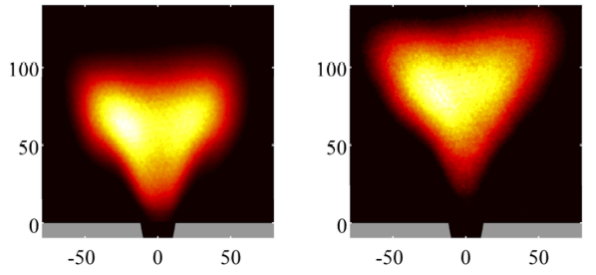

(a) ϕ=0.95, S=0.9, P=19.3 kW, T_{ad}=2200 K (b) ϕ=0.8, S=0.9, P=12.4 kW, T_{ad}=2010 K

Figure 6: CH_4/air flames at the same $U_b/S_L = 55$

lifted V-shape flame appears are shifted to smaller values than $S \simeq 0.75$ for a $P = 12.5\ kW$ flame. These experiments confirm that the swirl number S is one of the main parameter controlling the topology of these CO_2- and N_2-diluted swirling flames.

Effects of dilution

Effects of the diluant composition

Schroll *et al.* [17] found that the the adiabatic flame temperature T_{ad} has a major influence on the dynamic stability of the swirled combustor they studied when N_2 is replaced by CO_2. Diluted flames featuring the same adiabatic flame temperature are compared in this section. For a CH_4/air flame at $\phi = 0.95$ this temperature is $T_{ad} = 2200$ K. The same flame temperature is reached for a $X_{CO_2} = 68\%$ diluted oxyflame featuring the same equivalence ratio as CH_4/air flame. For air combustion, the N_2 is fixed $X_{N2} = 79\%$, indicating that for the same adiabatic flame temperature and the same power, the mixture bulk flow injection velocity U_b of the $CH_4/O_2/CO_2$ flame is much lower than the injection bulk velocity for air combustion.

Figures 3 and 4 show $CH_4/O_2/N_2$ and $CH_4/O_2/CO_2$ swirled flames at the same thermal power P=12.5 kW, same equivalence ratio $\phi = 0.95$ and the same adiabatic flame temperature T_{ad}. CO_2-diluted flames take the same shapes as N_2-diluted flames for similar values of the swirl number. This comparison was also conducted at different thermal powers, for different equivalence ratios and for different dilution rates. The operating ranges of the parameters are synthesized in Tab. 1. For experiments conducted at $P = 10$ kW with CO_2, the injection bulk velocity U_b of the combustible mixture was too small compared to the laminar burning velocity $U_b/S_L = 34$. These flames were too unsteady and eventually blew off. It was not possible to stabilize CO_2-diluted flames when $U_b/S_L < 34$ at ambient temperature injection conditions in our setup. N_2-diluted swirled flames could however be stabilized when $U_b/S_L < 34$. This confirms that CO_2-diluted flames are harder to stabilize than N_2-diluted flames [19].

When the thermal power is increased $P > 10$ kW, the ratio U_b/S_L is large enough to stabilize CO_2 and N_2-diluted flames. Observations are similar to those made at the reference power of P=12.5 kW and for $\phi = 0.95$. CO_2- and N_2-diluted flames featuring the same adiabatic flame temperature T_{ad} and the same swirl number S have almost the same topology even at a lower equivalence ratio and for different dilution rates.

These experiments confirm results of Shroll *et al.* [17]. In all cases explored, for injection Reynolds numbers lower than $Re < 30000$, CO_2- and N_2-diluted flames have the same structure when their adiabatic flame temperature T_{ad} and swirl numbers S are identical. N_2-diluted flames are however easier to stabilize at low equivalence ratios and high dilution rates. We also found out that it was easier to stabilize N_2-diluted flames with a V-shape when they are lifted away from the burner.

Influence of the U_b/S_L and T_{ad}

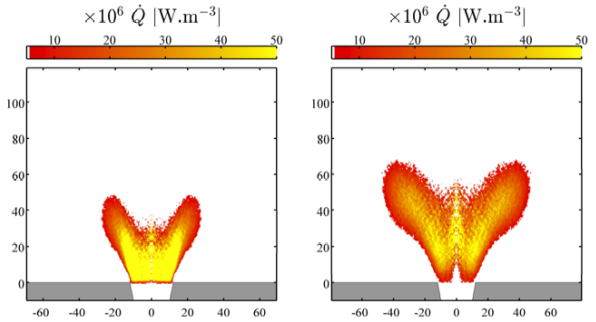

(a) ϕ=0.95, S=0.9, P=10 kW, U_b/S_L=28.5 (b) ϕ=0.95, S=0.9, P=20 kW, U_b/S_L=56.5

Figure 7: Abel deconvolution of CH_4/air flames at the same T_{ad}=2200 K

Flames with the same U_b/S_L ratio or adiabatic flame temperature T_{ad}, but at different thermal powers, swirl numbers and dilution rates were observed. These experiments indicate that the ratio U_b/S_L and adiabatic flame temperature barely affect the shape of the flame compared to modifications of the swirl number. Only a change of the swirl number led to a transition from a V-shaped to a tulip-shaped flame in Fig. 3. The quantities U_b/S_L and T_{ad} however affect the range of swirl numbers where the different topologies appear. The range of swirl numbers where the lifted V-shaped flame can be stabilized widens when U_b/S_L increases or when the adiabatic flame temperature T_{ad} decreases. These parameters need also to be in the right ranges. When $T_{ad} < 1800\ K$ for N_2-diluted mixtures or $T_{ad} < 1900\ K$ for CO_2-diluted mixtures, it was not possible to stabilize swirled flames for a long duration after ignition. This was also the case when $U_b/S_l < 34$ for CO_2-diluted mixtures. N_2-diluted flames could be stabilized for all U_b/S_L ratios explored.

Images in Fig. 6 show flames featuring the same U_b/S_L ratio and swirl number $S = 0.9$, but for different adiabatic flame temperature: $T_{ad} = 2200\ K$ in Fig. 6(a) and $T_{ad} = 2010\ K$ in Fig. 6(b). A change in the adiabatic flame temperature alters the position of the flame. For lower adiabatic flame temperature, the size of the flame also changes For a constant U_b/S_L and a constant swirl number, a decrease of the adiabatic flame temperature leads to an increase of the flame volume and finally results in a liftoff of the flame root above the injector, until the flame loses its shape and eventually blows off.

In Figs. 5 and 7, the adiabatic flame temperature and the swirl number are kept constant, and the ratio U_b/S_L is varied. When U_b/S_L changes from 28.5 to 56.5, there are no obvious change of the flame shape in Fig. 7. As more gases are injected at $P = 20$ kW, the flame is however longer than at $P = 12.5$ kW, but their topology is the same. When U_b/S_L increases from 66 in Fig. 5(b) to 73 in Fig. 5(a), major modifications of the flame topology are observed. These results demonstrate that there is no direct correlation between the ratio U_b/S_L and the

shape taken by the swirled flames when the combustor is operated at fixed adiabatic flame temperature and swirl number. Depending on the value of the adiabatic flame temperature T_{ad}, a change of U_b/S_L may or may not have an effect on the flame topology. The ratio U_b/S_L does not seem to be a relevant parameter to take into account when studying the topology of swirling flames.

Conclusion

It was shown that it is possible to anticipate the shape of $CH_4/O_2/CO_2$-diluted swirled flames by examining the topology of CH_4/air flames provided that the injector geometry, swirl number and adiabatic flame temperature of the combustible mixtures are the same. CO_2-diluted flames are however less stable than N_2-diluted flames for the range of operations explored. This study was conducted for injection Reynolds numbers limited to $Re < 20000$ with aerodynamically stabilized flames without the help of a central bluff body. In a future work, higher values of the injection Reynolds number will be considered. This study also emphasized the major influence of the diverging quarl at the burner outlet. The ranges of adiabatic flame temperatures T_{ad} and ratios U_b/S_L allowing the stabilization of swirled flames also differ for N_2- and CO_2-diluted flames. These parameters also influence the transitions where the different flame patterns take place. When T_{ad} decreases, V-shaped flames are easier to lift-off above the injector and the flame becomes bigger. It is also easier to lift-off V-flames for high values of U_b/S_L. Knowing the value of U_b/S_L however does not allow to directly determine the type of flame pattern.

From an practical point of view, these results indicate that transformation of a swirled burner operated with premixed methane air mixtures to oxycombustion diluted by CO_2 can be realized by matching the swirl number S and the adiabatic flame temperature T_{ad} of the combustible mixture without modifying the injector. One then also needs to check that T_{ad} and U_b/S_L are in the range of stability for $CH_4/O_2/CO_2$ flames. Due to the different thermal properties of CO_2 and N_2, heat transfers will necessarily differ between both diluents even for the same adiabatic flame temperature. Therefore, for applications where the thermal transfers need to be controlled, the impact of heat transfer on flame topology has to be addressed.

Acknowledgements

This work is supported by the Air Liquide, Ecole Centrale Paris and CNRS Chair on oxycombustion and heat transfer for energy and environment and by the OXYTEC project (ANR-12-CHIN-0001) from l'Agence Nationale de la Recherche. We also would like to thank the technical staff of EM2C for their assistance during the design and construction of the experimental setup.

References

[1] N. Perrin, R. Dubettier, F. Lockwood, P. Court, J.-P. Tranier, C. Bourhy-Weber, M. Devaux, Energy Procedia 37 (2013) 1389 – 1404.

[2] D. Cieutat, I. Sanchez-Molinero, R. Tsiava, P. Recourt, N. Aimard, C. Prébendé, Energy Procedia 1 (2009) 519 – 526.

[3] N. Perrin, C. Paufique, M. Leclerc, Energy Procedia 63 (2014) 524 – 531.

[4] B. Buhre, L. Elliott, C. Sheng, R. Gupta, T. Wall, Progress in Energy and Combustion Science 31 (2005) 283 – 307.

[5] N. Syred, Progress in Energy and Combustion Science 32 (2006) 93 – 161.

[6] N. Syred, J. Beér, Combustion and Flame 23 (1974) 143 – 201.

[7] S. N. Gupta A. K., Lilley D. G., Swirl flows, Abacus Press, Tunbridge Wells, Kent, England, 1984.

[8] D. Durox, J. P. Moeck, J.-F. Bourgouin, P. Morenton, M. Viallon, T. Schuller, S. Candel, Combustion and Flame 160 (2013) 1729 – 1742.

[9] H. C. Mongia, AIAA Paper 5526 (2011).

[10] F. Vega, F. Benjumea, B. Navarrete, E. Portillo, Fuel 139 (2015) 637 – 645.

[11] F. Halter, F. Foucher, L. Landry, C. Mounaïm-Rousselle, Combustion Science and Technology 181 (2009) 813–827.

[12] A. Mazas, D. A. Lacoste, T. Schuller, in: ASME Turbo Expo 2010: Power for Land, Sea, and Air, American Society of Mechanical Engineers, pp. 411–421.

[13] P. Glarborg, L. L. B. Bentzen, Energy & Fuels 22 (2008) 291–296.

[14] C. Liu, G. Chen, N. Sipöcz, M. Assadi, X. Bai, Applied Energy 89 (2012) 387 – 394.

[15] S. W. Jung, J. Park, O. B. Kwon, Y. J. Kim, S. I. Keel, J. H. Yun, I. G. Lim, Fuel 136 (2014) 69 – 78.

[16] H. Kobayashi, H. Hagiwara, H. Kaneko, Y. Ogami, Proceedings of the Combustion Institute 31 (2007) 1451 – 1458.

[17] A. P. Shroll, S. J. Shanbhogue, A. F. Ghoniem, Journal of Engineering for Gas Turbines and Power 134 (2012) 051504–051504.

[18] S. Seepana, S. Jayanti, Fuel 93 (2012) 75 – 81.

[19] A. Amato, B. Hudak, P. D'Carlo, D. Noble, D. Scarborough, J. Seitzman, T. Lieuwen, Journal of Engineering for Gas Turbines and Power 133 (2011) 061503–061503.

[20] K. Lee, H. Kim, P. Park, S. Yang, Y. Ko, Fuel 106 (2013) 682 – 689.

[21] L. Tay Wo Chong, T. Komarek, M. Zellhuber, J. Lenz, C. Hirsch, W. Polifke, in: Proc. Of European Comb. Meeting (2009).

[22] T. Guiberti, D. Durox, P. Scouflaire, T. Schuller, Proceedings of the Combustion Institute 35 (2015) 1385 – 1392.

[23] N. Darabiha, Combustion Science and Technology 86 (1992) 163–181.

[24] G. P. Smith, D. M. Golden, M. Frenklach, N. W. Moriarty, B. Eiteneer, M. Goldenberg, C. T. Bowman, R. K. Hanson, S. Song, W. C. Gardiner Jr, et al., Gri-mech 3.0, 1999.

[25] N. Docquier, S. Candel, Progress in Energy and Combustion Science 28 (2002) 107 – 150.

[26] L. M. Smith, D. R. Keefer, S. Sudharsanan, Journal of Quantitative Spectroscopy and Radiative Transfer 39 (1988) 367 – 373.

[27] P. Palies, D. Durox, T. Schuller, S. Candel, Combustion and Flame 157 (2010) 1698 – 1717.

[28] F. Guethe, D. Guyot, G. Singla, N. Noiray, B. Schuermans, Applied Physics B 107 (2012) 619–636.

[29] K. T. Kim, J. G. Lee, H. J. Lee, B. D. Quay, D. A. Santavicca, Journal of Engineering for Gas Turbines and Power 132 (2010) 041502–041502.

[30] A. F. Ghoniem, O. M. Knio, Symposium (International) on Combustion 21 (1988) 1313 – 1320.